

APPENDIX B
EXAMPLE OF A LATENT DEBRIS SURVEY

In an effort to quantify the amount of latent debris located on vertical surfaces, samples were taken of latent debris on vertical surfaces inside containment of a volunteer plant. The surfaces surveyed appeared to be clean. However, the surfaces were not perfectly clean, as evidenced by the results of the survey. Samples were taken using Maslins (commonly used for decontamination of floors). Four samples were collected: two from the containment liner and two from the internal concrete structure. Photographs of the survey process and the Maslins are presented in Figures B-1 through B-5. The results of the survey are contained in Table B-1.

Table B-1. Results of Survey of Vertical Surfaces Inside Containment

Elevation ft	Location --	Sample Area ft²	Net Weight g	Estimated Collection Efficiency %	Debris Concentration g/1000 ft²
905	Liner	120	1.95	90	18
808	Liner	216	1.32	90	7
860	Interior wall	70	0.21	90	3
905	Interior wall	168	0.95	90	6

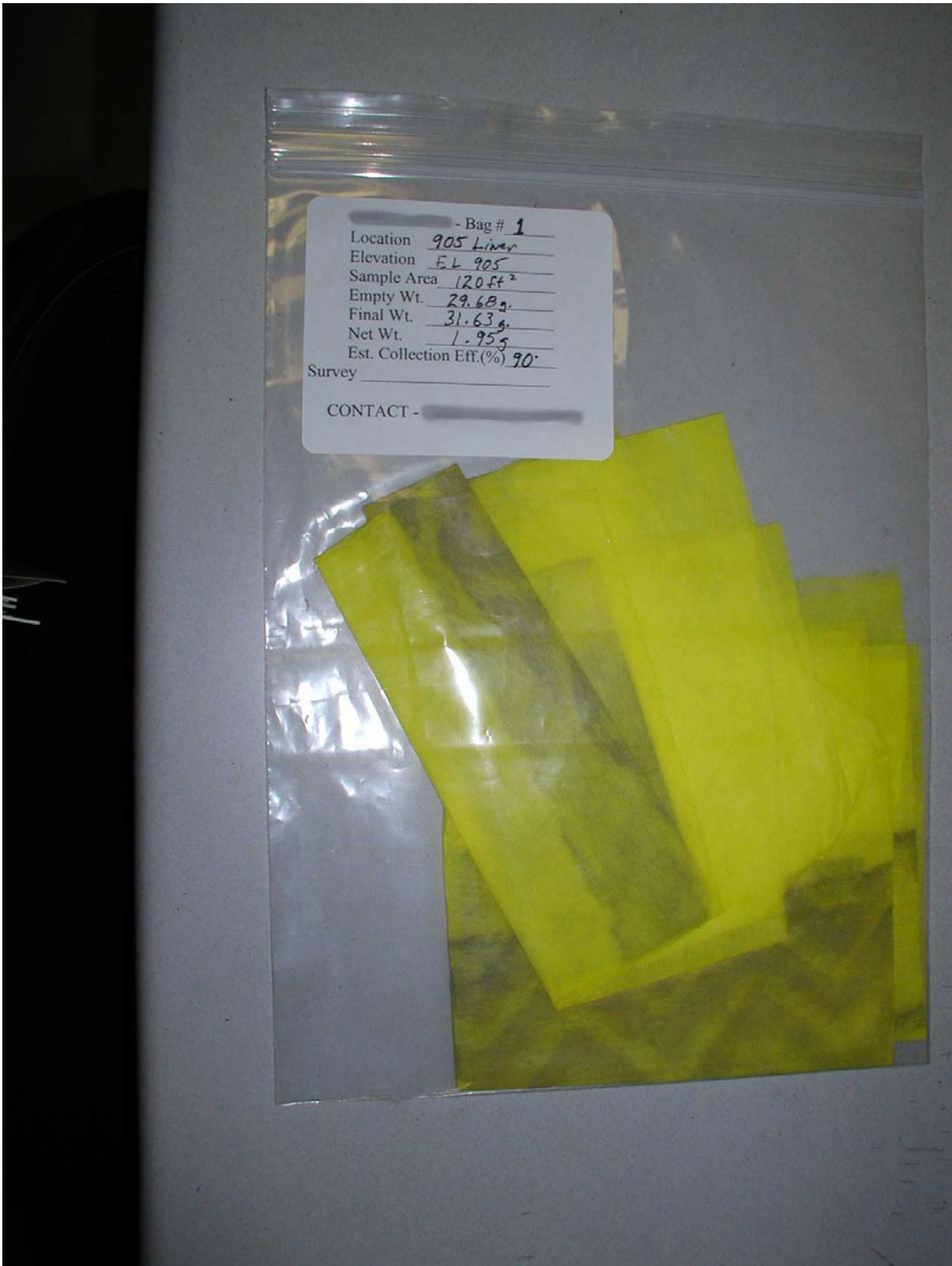
The measured debris concentrations for the containment liner ranged from 7 to 18 grams per 1,000 square feet. The surface area of the liner in the volunteer plant is approximately 110,000 square feet, including the dome. Assuming 18 grams per 1,000 square feet, the total quantity of latent debris on the coated steel liner is calculated to be less than 5 pounds:

$$\left(\frac{18\text{g}}{1,000\text{ ft}^2}\right) \times (110,000\text{ ft}^2) \times \left(\frac{2.205 \times 10^{-3}\text{ lb}}{1\text{g}}\right) = 4.4\text{ lb}$$

The measured debris concentrations for the coated concrete interior wall ranged from 3 to 6 grams per 1,000 square feet. Vertical concrete surface areas would be comparable to the liner. Assuming 6 grams per 1,000 square feet and a total surface area of 110,000 square feet, the total quantity of latent debris on the coated internal structures is calculated to be less than 2 pounds:

$$\left(\frac{6\text{g}}{1,000\text{ ft}^2}\right) \times (110,000\text{ ft}^2) \times \left(\frac{2.205 \times 10^{-3}\text{ lb}}{1\text{g}}\right) = 1.5\text{ lb}$$

The data for the vertical coated concrete were comparable to data for the main floors taken after cleaning during containment close-out. The results of the survey indicate that areas that look clean, including vertical surfaces, represent only a small contribution to the latent debris source term.



1

2

Figure B-1. Photograph of Sample Collected from Containment Liner



1

2

Figure B-2. Photograph of Sample Collected from Containment Liner



1

2

Figure B-3. Photograph of Sample Collected from Coated Concrete Wall



1

2

Figure B-4. Photograph of Sample Collected from Coated Concrete Wall



1

2

Figure B-5. Photograph of Collection Process

APPENDIX C COMPARISON OF NODAL NETWORK AND CFD ANALYSIS

C.1 VELOCITY/FLOW CALCULATION

The results of the open-channel network nodal model for the volunteer plant compare very favorably with the computational fluid dynamics (CFD) analysis, generally providing calculated flow values with an error of less than 10 percent of the total recirculation flow. The error is calculated by subtracting the nodal network calculated flow from the CFD calculated flow, and dividing the result by the total recirculation flow. Calculating the error in this manner purposely masks differences that are significant when viewed in absolute terms, but insignificant when normalized considering the total recirculation flow (and hence in the ability to move debris). For example, for channel -167 in Table C-1, the differences between the two values are fairly large, but when normalized to the recirculation flow, the differences are only 5 percent. Such differences should be expected, particularly when the flow pattern is a ring and divides at some point in the ring to move in one direction. The bulk flow rate velocities at these points are expected to be relatively small and thus, the overall ability to transport will be insignificant.

To address the inaccuracies of the low-flow regime calculations, uncertainty within the input flow distribution values, and potential errors within the CFD modeling process, it is recommended that 10 percent of the total recirculation flow, as a minimum, should be added to the calculated flow rates and sensitivity calculations should be based on that biased value to identify particular aspects that could significantly influence the results.

A second concern that arises is that the debris transported from a region where flow is calculated to be in the reverse direction (i.e., reversed from the CFD model) may be influenced by a debris-limiting obstacle in the calculated direction versus the other. For example, see channel 156 below. This concern is, however, mitigated by the fact that the bulk velocities are sufficiently low in these low-flow regions that the debris inventory normally susceptible to flow-induced movement will generally not be transported regardless of the calculated direction. Therefore, it is judged acceptable that these low-flow channels may be calculated to be flowing in the reverse direction.

1

Table C-1. Error Calculations

Channel ID (Node to Node)	Channel Area (ft ²)	Flow Map Liquid Flow Rate (gpm)	CFD Calculated Flow Rate (gpm)	Flow Map Calculated Velocity (ft/sec)	CFD Calculated Velocity (ft/sec)	Percent Error: Flow Map versus CFD (Δ Flow/Total Flow)
Channel 156 (Node 1 to 9)	73.4	-583.7	1035	0.018	0.034	7.7%
Channel -167 (Node 9 to 10)	36.2	220.3	1297	0.014	0.0842	5.1%
Channel -130 (Node 10 to 7)	25.3	6791.3	7497	0.598	0.66	3.4%
Channel -50 (Node 6 to 7)	58.3	12544.4	11929	0.479	0.4567	2.9%
Channel -20 (Node 5 to 6)	68.2	9254	11120	0.302	0.399	8.9%
Channel 0 (Node 4 to 5)	49.4	7261.3	6569	0.327	0.2962	3.3%
Channel 33 (Node 3 to 4)	92.3	5289	5012	0.128	0.121	1.3%
Channel 110 (Node 1 to 3)	67.4	3270.7	1695	0.108	0.0569	7.5%

2

3 C.2 LIMITATIONS

4 The following limitations are acknowledged for the open-channel flow nodal network approach.
5 Each of the limitations is addressed in subsequent paragraphs or sections.

6 C.2.1 Filling Operations

7 The method does not attempt to analyze the movement of debris during filling operations but is
8 directed only at debris motion subsequent to initiation of the post-accident recirculation phase.
9 The rationale for focus on the recirculation phase is that this is the time frame when there is a
10 forced and general fluid movement toward the sump screens that overwhelms any debris action
11 during fill (beyond initial debris distribution). Further, if filling action were isolated to a specific
12 and limited location in containment, there could be a general movement from the source to the
13 sump during filling. However, as demonstrated in the volunteer plant input and as would be
14 expected for containments generally, containment filling is driven by break flow and spray flow
15 that would not be a single-source delivery. Therefore, this approach is focused on analysis of
16 debris action upon initiation of recirculation.

17 C.2.2 Turbulent Flow

18 The nodal network approach does not calculate turbulent effects or vertical velocities. These are
19 primarily localized effects and are attenuated with the proper levels of conservatism and the
20 subsequent effects of the velocity fields to final destination. The exception to the attenuation is
21 the insulation erosion effects that result from local turbulences. These are minimized, however,
22 with proper attention to debris generation efforts. See Section C.3.

23 Within the regions with major flow inputs, for example in the volunteer plant where the loop
24 compartments empty into the main flow (i.e., channels -130 and channel -50), turbulence will be

1 created as the flow turns to align with channel flow or at points where flow input is delivered to
2 the top layer of the flooded levels and turns to align with channel flow. Within these local regions
3 and for other major flow changes due to flow rate changes or obstacles, turbulence is generated
4 and consequently, the effects on debris within the area should be factored into debris inventory.

5 **C.2.2.1 Vertical Turbulent Velocity**

6 A measure of the degree to which turbulence should be factored into the evaluation of debris
7 movement is an estimate of the percentage of CFD calculated flow rates that have a sufficient
8 vertical component of velocity to cause the overall velocity to become a contributor to debris
9 transport. If a conservative value of 0.1 ft/sec is considered as a threshold velocity, then less than
10 3 percent of the CFD points (at the 0.6-meter level) are moved from a threshold velocity below
11 0.1 ft/sec to above 0.1 ft/sec when the vertical velocity component is considered, and for which
12 the vertical component is a significant constituent of the total flow (greater than 20 percent).
13 These points would be expected to be located close to the major flow input points. The 0.1-ft/sec
14 threshold velocity is based on the minimum incipient tumbling velocity reported in
15 Reference C-2 of 0.12 ft/sec for any type of insulation tested. Note that if the vertical component
16 of velocity is considered at the 0.1-meter level rather than the 0.6-m level, only 0.3 percent of the
17 CFD points meet the above criteria. In other words, the closer to the floor the insulation is likely
18 to be located (and the farther from the point source), the vertical constituent of local velocity is
19 less likely to influence the ability of the bulk flowrate to move insulation toward the containment
20 sump. Effectively, it is not judged necessary to consider the vertical constituent to transport
21 velocity when evaluating channel flow transport velocities.

22 **C.2.2.2 Horizontal Turbulent Velocity**

23 A second influence of turbulent local flow is the increased local horizontal velocities due to
24 major inputs to channel flow. Examination of the CFD computational maps (See Figure 4-2 in
25 subsection 4.2.4.2) confirms this aspect of point source flow additions to the channel flow. The
26 magnitude of the influence from incoming flows is proportional to the magnitude of the influx of
27 flow rate but inversely proportional to the prevailing bulk velocity. Examining channel 156
28 assists in the evaluation of this factor. The CFD calculated flow rate through this channel (taken
29 at azimuth 156 degrees where the flow is relatively stable across the azimuth) is 0.034 ft/sec
30 (0.0104 m/sec). The major influx of flow is at azimuth 140 degrees. A review of the velocity
31 mapping indicates that the local velocity at the influx source point increases above 0.1 ft/sec
32 (0.0304 m/sec) and therefore debris that resides in this area could be transported and should be
33 taken into consideration. There are, however, additional factors that influence the final
34 determination. The following is the suggested approach for evaluating these local elevated
35 horizontal velocity regions.

- 36 • If the bulk velocity for the channel exceeds the debris transport incipient velocity,
37 the debris is transported and need not be evaluated further.
- 38 • If there is a channel between the influx point and the containment sump or a
39 significant area between the influx point and the sump where the bulk velocity is
40 less than the incipient velocity for the debris inventory, the debris may be moved

1 initially but would resettle and need not be considered in the overall debris
2 evaluation. Note that the settling velocity per Reference C-2 varies from 0.12 ft/sec
3 for low density debris to 0.44 ft/sec for higher-density debris and thus, the area
4 required for settling need not be extensive, since most debris will slide or tumble
5 along the floor and settle quickly.

- 6 • For those influx source points that do not satisfy either of the above criteria, the
7 debris residing in the area affected by the point sources should be considered in the
8 debris transported to the sump using the following approach.

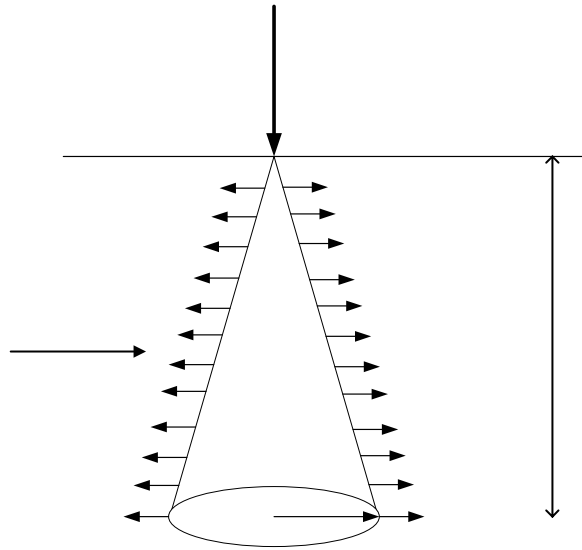
- 9 – Determine the difference between the local bulk velocity and the velocity of
10 incipient motion for the debris inventory (Reference C-2). This is termed the
11 “velocity boost.”
- 12 – The point source will have a cone of influence emanating from the source
13 and plunging into the flooded volume. The size of the cone for which the
14 local velocity is boosted above incipient velocity will depend primarily on the
15 volumetric flow rate.
- 16 – Calculate the floor area for which the velocity is boosted due to the incoming
17 flow by assuming that the flow velocity through the lateral area of the cone is
18 equal to the required boost velocity. That is, maximize the floor area affected
19 by calculating a cone for which the lateral area equals the area necessary to
20 yield a calculated velocity equal to the required boost velocity, as shown in
21 Figure C-1.

$$22 \quad V_B = Q/A$$

- 23 – Calculate the required floor radius to yield the lateral area.

$$24 \quad A = 1/2 (2\pi r) \times h$$

- 25 – The debris within the floor area with a radius r should be factored into the
26 inventory of debris transported to the sump.



1

2

Figure C-1. Illustration of Point Source Calculations

3

C.3 PRIOR KNOWLEDGE OF CFD RESULTS

4 The open-channel flow nodal network model development applied knowledge gained from CFD
 5 “Containment Pool Flow Analysis” for the volunteer plant. The cooperation of Los Alamos
 6 National Laboratory personnel is gratefully acknowledged in developing the CFD model and
 7 providing supporting data, drawings, and background to better understand the results of the CFD
 8 model (Reference C-1) as applicable to channel flow modeling. Although the CFD results
 9 enhanced understanding of containment sump recirculation flow, including definition of channels
 10 as well as the refinement of the analysis technique, it must be understood that the guidelines
 11 provided for generation of a channel network in subsection 4.2.4.1 of this report were developed
 12 to alleviate the need for that specific, detailed knowledge. A CFD model of the containment floor
 13 is not explicitly required for successful development of a channel flow model, provided that
 14 guidelines are implemented and the conservatism applied.

15

C.4 REFERENCES

16 C-1. Los Alamos National Laboratory, “Volunteer Plant Containment Pool Flow Analysis,”
 17 David DeCroix, Nuclear Design and Risk Analysis Group, presented at NRC Public
 18 Meeting, March 5, 2003.

19 C-2. NUREG/CR-6808, “Knowledge Base for the Effect of Debris on Pressurized Water
 20 Reactor Emergency Core Cooling Sump Performance,” U.S. Nuclear Regulatory
 21 Commission, February 2003.

B

Table D-1. Normalized Isobar Map for Insulation Destruction Pressures of Interest

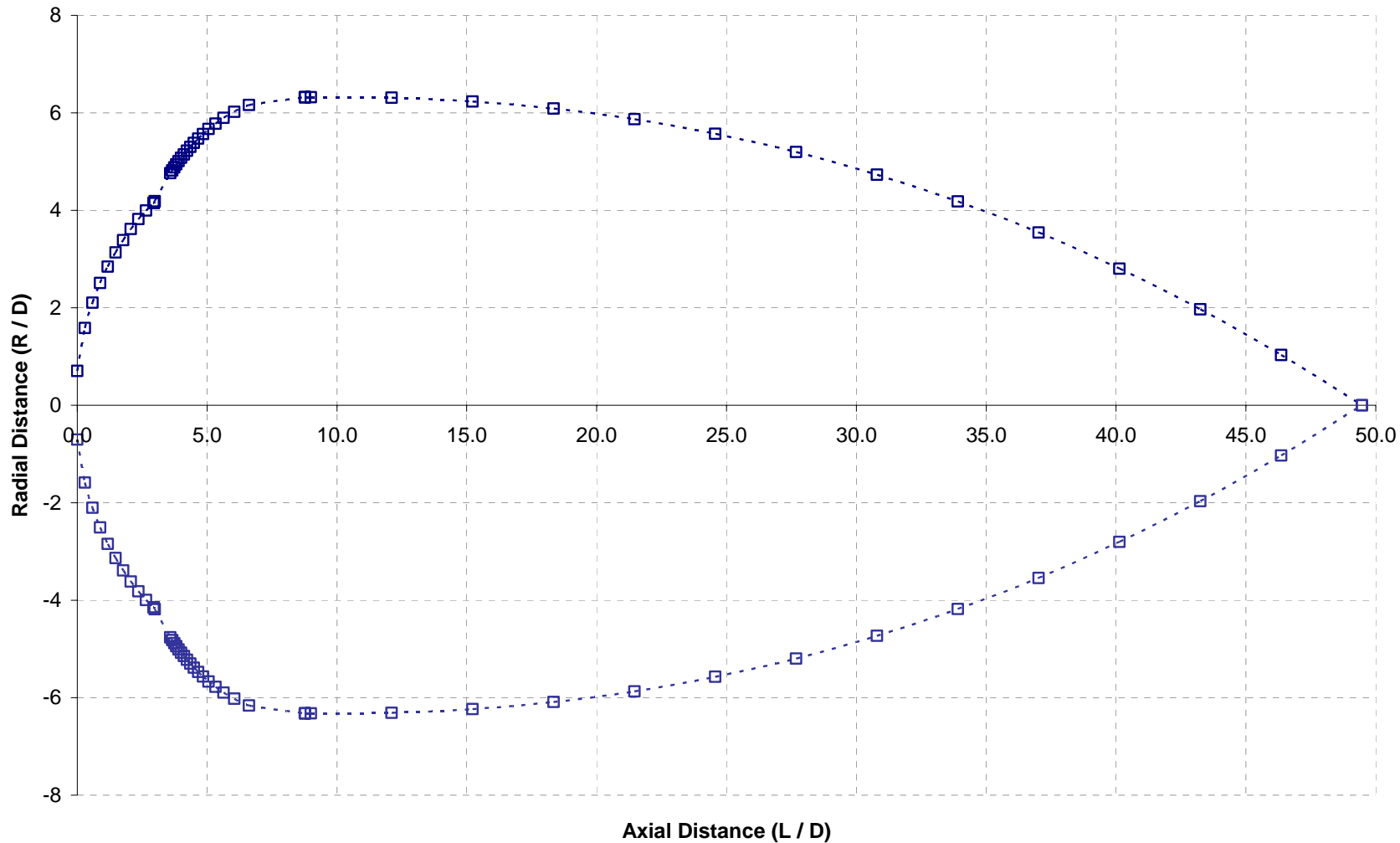
Length (L/D)	Isobar Diameter (D_{isobar}/D_{break})									
	4 psi	6 psi	10 psi	17 psi	24 psi	40 psi	50 psi	64 psi	150 psi	190 psi
0.0	1.41	1.41	1.41	1.41	1.41	1.41	1.41	1.41	1.41	1.41
0.3	3.35	3.28	3.17	3.02	2.89	2.67	2.55	2.40	1.73	1.48
0.6	4.50	4.39	4.21	3.97	3.77	3.42	3.23	3.00	1.94	1.56
0.9	5.39	5.24	5.01	4.70	4.45	3.99	3.75	3.44	2.07	1.57
1.2	6.14	5.96	5.68	5.31	5.00	4.45	4.15	3.79	2.13	1.52
1.5	6.80	6.59	6.27	5.83	5.47	4.82	4.48	4.06	2.12	1.42
1.8	7.38	7.15	6.78	6.28	5.87	5.13	4.75	4.26	2.06	1.26
2.1	7.91	7.65	7.23	6.67	6.22	5.38	4.95	4.41	1.93	1.03
2.4	8.39	8.10	7.63	7.01	6.50	5.58	5.09	4.49	1.73	0.73
2.7	8.82	8.50	7.99	7.30	6.74	5.71	5.17	4.51	1.45	0.34
2.9	9.22	8.86	8.30	7.53	6.92	5.78	5.19	4.45	1.08	0.00
3.0	9.23	8.87	8.30	7.54	6.92	5.78	5.19	4.45	1.06	0.00
3.6	10.74	10.29	9.52	8.42	7.50	5.77	4.85	3.70	0.00	0.00
3.7	10.88	10.43	9.64	8.50	7.55	5.74	4.78	3.57	0.00	0.00
3.7	11.02	10.56	9.76	8.59	7.59	5.71	4.70	3.43	0.00	0.00
3.8	11.17	10.71	9.89	8.67	7.64	5.66	4.61	3.27	0.00	0.00
3.9	11.32	10.85	10.02	8.76	7.69	5.61	4.49	3.08	0.00	0.00
4.0	11.48	11.01	10.15	8.85	7.73	5.54	4.36	2.86	0.00	0.00
4.1	11.65	11.17	10.30	8.95	7.77	5.46	4.20	2.60	0.00	0.00
4.2	11.83	11.35	10.44	9.04	7.80	5.35	4.01	2.30	0.00	0.00
4.4	12.02	11.53	10.60	9.14	7.83	5.21	3.77	1.92	0.00	0.00
4.5	12.23	11.72	10.77	9.24	7.85	5.04	3.48	1.47	0.00	0.00
4.7	12.45	11.93	10.94	9.34	7.85	4.82	3.11	0.90	0.00	0.00
4.8	12.70	12.16	11.13	9.43	7.84	4.53	2.64	0.17	0.00	0.00
5.1	12.97	12.42	11.33	9.52	7.80	4.14	2.02	0.00	0.00	0.00
5.3	13.28	12.70	11.55	9.60	7.71	3.61	1.18	0.00	0.00	0.00
5.6	13.64	13.02	11.79	9.66	7.56	2.86	0.00	0.00	0.00	0.00

Table D-1. Normalized Isobar Map for Insulation Destruction Pressures of Interest (Cont'd)

Length (L/D)	Isobar Diameter (D_{isobar}/D_{break})									
	4 psi	6 psi	10 psi	17 psi	24 psi	40 psi	50 psi	64 psi	150 psi	190 psi
6.0	14.07	13.40	12.05	9.67	7.28	1.75	0.00	0.00	0.00	0.00
6.6	14.61	13.85	12.32	9.58	6.77	0.00	0.00	0.00	0.00	0.00
8.8	16.18	15.00	12.64	8.52	4.40	0.00	0.00	0.00	0.00	0.00
9.0	16.23	15.03	12.65	8.47	4.29	0.00	0.00	0.00	0.00	0.00
12.1	16.88	15.46	12.62	7.66	2.70	0.00	0.00	0.00	0.00	0.00
15.2	17.47	15.81	12.47	6.63	0.79	0.00	0.00	0.00	0.00	0.00
18.3	18.02	16.07	12.18	5.36	0.00	0.00	0.00	0.00	0.00	0.00
21.5	18.50	16.25	11.74	3.85	0.00	0.00	0.00	0.00	0.00	0.00
24.6	18.92	16.33	11.14	2.07	0.00	0.00	0.00	0.00	0.00	0.00
27.7	19.28	16.31	10.39	0.02	0.00	0.00	0.00	0.00	0.00	0.00
30.8	19.57	16.20	9.47	0.00	0.00	0.00	0.00	0.00	0.00	0.00
33.9	19.79	15.98	8.37	0.00	0.00	0.00	0.00	0.00	0.00	0.00
37.0	19.93	15.65	7.08	0.00	0.00	0.00	0.00	0.00	0.00	0.00
40.1	20.00	15.20	5.61	0.00	0.00	0.00	0.00	0.00	0.00	0.00
43.2	19.99	14.64	3.94	0.00	0.00	0.00	0.00	0.00	0.00	0.00
46.4	19.90	13.95	2.06	0.00	0.00	0.00	0.00	0.00	0.00	0.00
49.5	19.72	13.14	0.00	0.00	0.00	0.00	0.00	0.00	0.00	0.00
52.6	19.46	12.19	0.00	0.00	0.00	0.00	0.00	0.00	0.00	0.00
55.7	19.10	11.11	0.00	0.00	0.00	0.00	0.00	0.00	0.00	0.00
58.8	18.65	9.88	0.00	0.00	0.00	0.00	0.00	0.00	0.00	0.00
61.9	18.10	8.51	0.00	0.00	0.00	0.00	0.00	0.00	0.00	0.00
65.0	17.46	7.00	0.00	0.00	0.00	0.00	0.00	0.00	0.00	0.00
68.1	16.71	5.32	0.00	0.00	0.00	0.00	0.00	0.00	0.00	0.00
71.3	15.85	3.49	0.00	0.00	0.00	0.00	0.00	0.00	0.00	0.00
74.4	14.89	1.50	0.00	0.00	0.00	0.00	0.00	0.00	0.00	0.00
77.5	13.81	0.00	0.00	0.00	0.00	0.00	0.00	0.00	0.00	0.00
80.6	12.62	0.00	0.00	0.00	0.00	0.00	0.00	0.00	0.00	0.00
83.7	11.32	0.00	0.00	0.00	0.00	0.00	0.00	0.00	0.00	0.00

**Table D-1. Normalized Isobar Map for Insulation Destruction Pressures of Interest
(Cont'd)**

Length (L/D)	Isobar Diameter (D_{isobar}/D_{break})									
	4 psi	6 psi	10 psi	17 psi	24 psi	40 psi	50 psi	64 psi	150 psi	190 psi
86.8	9.89	0.00	0.00	0.00	0.00	0.00	0.00	0.00	0.00	0.00
89.9	8.34	0.00	0.00	0.00	0.00	0.00	0.00	0.00	0.00	0.00
93.1	6.66	0.00	0.00	0.00	0.00	0.00	0.00	0.00	0.00	0.00
96.2	4.85	0.00	0.00	0.00	0.00	0.00	0.00	0.00	0.00	0.00
99.3	2.92	0.00	0.00	0.00	0.00	0.00	0.00	0.00	0.00	0.00
102.4	0.84	0.00	0.00	0.00	0.00	0.00	0.00	0.00	0.00	0.00
105.5	0.00	0.00	0.00	0.00	0.00	0.00	0.00	0.00	0.00	0.00



1

2

Figure D-1. Normalized Isobar Map for 10 psi Stagnation Pressure

APPENDIX E ADDITIONAL INFORMATION REGARDING DEBRIS HEAD LOSS

E.1 BACKGROUND

The head loss across a screen is highly dependent on the size and shape of the insulation debris reaching the screen. These debris characteristics depend on a variety of factors, including the type and manufacturer of the material (e.g., Nukon versus mineral wool versus Thermal-Wrap); plant aging effects such as the duration of exposure to high temperatures; the mode of transport (blowdown or washdown) to the recirculation pool; and the recirculation pool agitation at the time of the materials transport (e.g., chugging or falling water). For example, fiber debris may vary in size from individual fibers, typically a few millimeters in length, to shreds or small pieces that retain some of the original structure of the insulation blankets.

Nearly all of the suspended fibrous and metallic insulation debris approaching the strainer will be trapped by the strainer, except for a small quantity of finely destroyed debris (e.g., small individual fibers) that may pass through the strainer during the early stages of bed formation. During these early stages, the debris beds would be very thin and have a nonuniform thickness. In extreme cases, the debris bed may result in a partially covered strainer with open voids until more debris materials are transported. Initially, such beds may not have the required structure or strength to filter the particulate debris, especially particulates that are a few microns in size. As a result, most particulate debris approaching the strainer during these early stages will most likely penetrate the strainer and circulate through the reactor core region. The concerns arising from this consideration are known as “downstream effects” and are addressed in Section 7.3.

The non-uniformity of the bed during its initial formation may result in a redistribution of incoming flow, with more flow through the open areas where the flow resistance is lower. As a result of this redistribution, the newly arriving debris will be carried to the open areas of the strainer where they would be deposited. With time, continuous addition of debris in this manner will ultimately lead to formation of a thin, uniform debris bed on the strainer surface.

Some PWRs have quiescent pools (i.e., low-turbulence pools) and low approach velocities so that some or all of the material may not be transported to the screens. The material (particularly paint and RMI) that is transported near the floor may tend to accumulate near the front of the vertical or inclined screens. These factors should be considered in the development of the actual debris loads to which the screen will be subjected.

As the debris bed thickness increases, it acquires the required structure to commence filtering particulate debris passing through it. Filtration efficiencies close to 100 percent may be possible for larger particulates such as paint chips and concrete dust, but efficiencies on the order of 25 to 50 percent have been reported for filtration of particles ranging in size from 1-10 μm . As such, the quantity of particulate debris filtered by the fiber bed and, consequently, the head loss across the strainer (which is an increasing function of both the amount of debris trapped on the strainer and its geometry) are strong functions of the size distribution of the particulate debris reaching

1 the strainer. This also brings into focus the important role played by filtration efficiency in
2 estimating the head loss.

3 The head loss incurred during the debris bed buildup and the time at which such head loss may
4 exceed the available NPSH margin are important factors in design considerations and in planning
5 for mitigating actions. The rate and magnitude of head loss increase will be influenced by the
6 following factors:

- 7 • Amounts of various types of debris reaching the strainer and their rate of transport
8 at any given time.
- 9 • Size distribution and type of debris reaching the strainer.
- 10 • Filtration efficiency of the fibrous bed to trap particulate matter.
- 11 • ECCS flow rate and approach velocity.
- 12 • Recirculation pool temperature.
- 13 • Plant-specific considerations such as screen/strainer area, hole or mesh size, design,
14 and arrangement.

15 The detail to which such phenomena are modeled can significantly affect the calculated head loss
16 at any given time. Experience has shown the need to adopt a plant-specific transient analysis
17 model that incorporates all these considerations for performance evaluations. Moreover, mixtures
18 of fibrous materials and microporous insulation or calcium silicate may exhibit significantly high
19 head loss for relatively low amounts of fibrous material. Consequently, it is not appropriate to
20 extrapolate head loss obtained for one mixture of debris to another without taking into account
21 the debris characteristics. Any predictive calculations should be based on test data that provide
22 accurate debris characteristics of the constituents of the debris beds. Extrapolation of correlations
23 that do not factor the debris characteristics explicitly should not be practiced.

24 **E.2 SUMMARY OF SIGNIFICANT HEAD LOSS TESTS**

25 Table E-2 at the end of this section provides a compilation of the testing and data, results, and
26 pressure drop relationships developed by several organizations that have issued publicly
27 available head loss test information. In addition, Table E-2 provides a summary of experiments
28 and tests. The insulating materials used or simulated in these experiments consisted of:

29 Mineral wool (rockwool)

30 Low-density fiberglass (Nukon, Transco Thermal-Wrap)

31 High-density fiberglass

32 Caposil (Unibestos) (calcium silicate containing asbestos fibers)

- 1 Calcium silicate (diatomaceous earth, “Newtherm,” “Calosil”)
- 2 Insulation particulates (e.g., calcium silicate and alumina)
- 3 Reflective metallic insulation with stainless steel foils
- 4 Reflective metallic insulation with aluminum foils
- 5
 - Microporous insulation, including Min-K and Microtherm
- 6 Other debris materials included in some tests were:
- 7 Paint chips
- 8 Rust (iron oxide corrosion products)
- 9
 - Metallic particulates

10 Early Tests

11 Various techniques were used to generate insulation debris of representative sizes. For fibrous
 12 insulation, these included manual (hand) shredding, mechanical shredding (meat mincer, leaf
 13 shredder) and jet fragmentation (steamjets, waterjets, and airjets). The actual size class of the
 14 fibrous debris varied from as-fabricated blankets (without covers or scrims) to finely destroyed
 15 debris consisting of a significant quantity of individual fibers. Production techniques such as
 16 manual shearing and jet fragmentation were used for generation of nonfibrous insulation
 17 fragments used in the experiments (e.g., metallic insulation).

18 U.S. boiling water reactor (BWR) corrosion products were initially simulated using iron oxide
 19 particles that are larger than 75 μm owing to the lack of information related to size
 20 characteristics of the rust particles usually found in the BWR suppression pools. The U.S. BWR
 21 Owners’ Group (BWROG) later provided the information in Table E-1 that was used to size the
 22 corrosion products.

Table E-1. Size Distribution of Suppression Pool Sludge

Size, mm	% by weight
0-5	81
5-10	14
10-75	5

23
 24 The paint chips varied from 0.125 to 0.25 inches in size; and from 0.02 to 0.16 grams in weight.
 25 The size of the paint chips used in the experiments was based on engineering analyses provided
 26 by the BWROG for BWR containment coatings.

1 The head loss experiments listed in Table E-2 can be broadly categorized as 1) separate effects
2 experiments, and 2) small-scale strainer qualification tests. The focus of the separate effects tests
3 was to develop relationships that correlate strainer head loss to flow velocity and the amount of
4 debris on the strainer. The intent of the investigators was to use these relationships, together with
5 engineering judgment and assumptions regarding the debris generation and transport, to provide
6 the basis for design and sizing of the strainers. Typically, these tests employed a flat-plate
7 strainer and a closed test loop to conduct experiments. Note that the results from a once-through
8 column and closed-loop and open-loop recirculating experiments can produce significantly
9 different results if these experiments are not preplanned to separate such effects.

10 Typical data reported by the closed-loop experiments included head loss as a function of strainer
11 approach velocity and the quantity and type of debris added to the test loop. Some of the
12 European experimental data were reported in the form of coverage (kg/m^2) of insulation material
13 required to produce a head loss of 2 meters of water across the strainer as a function of velocity.
14 The material in Table E-2 includes the parameters and range studied in each experiment. The
15 head loss data were reported for theoretical bed thicknesses in the range of 3 mm to about 25 cm;
16 approach velocities in the range of 1 to 0.5 m/sec; at temperatures of 20°-25°C and 50°-55°C;
17 and for nominal sludge-to-fiber mass ratios in the range of 0 to 60. Considerable scatter exists in
18 head loss data from different sources. Careful examination of the experimental data suggests that
19 scattering can be attributed to the following:

- 20 • Variation in size classes of debris used in the experiments to simulate LOCA-
21 generated debris. (Typically, debris produced by manual methods is larger, that is,
22 NUREG/CR-6224 Classes 6 and 7, and resulted in lower pressure drops. On the
23 other hand, debris produced by mechanical methods and jet fragmentation was
24 much smaller and resulted in higher pressure drops. Further discussions related to
25 the effect of size class on the head loss across the strainer are presented in previous
26 sections.)
- 27 • Variation in the age of the fibrous insulation debris.
- 28 • Differences in experimental test loops.
- 29 • Differences in the range of experimental parameters. (For example, European
30 experiments were conducted at very low velocities, 1-10 cm/s, while the U.S.
31 experiments were conducted at much higher velocities, 5-50 cm/s.)
- 32 • The chosen method of correlating the data. (In most cases, purely empirical
33 relationships were sought to correlate the head loss data that were obtained for a
34 limited range of experimental parameters. This seriously limited extendibility of
35 these individual correlations beyond their original range of study.)

36 **Testing Performed After ~1995**

37 More recent tests and experiments were performed by different organizations either to provide a
38 basis for design of ECCS recirculation strainers and screens or a basis for regulation. The

1 organizations recognized the major shortcomings and limitations in the early testing programs
2 and devised the more recent ones to provide sufficiently detailed and proven information for the
3 intended purposes. Documents such as NUREG-6224 and the BWROG Utility Resolution Guide
4 (URG) are based on and/or refer to these recent investigations. Following are some of the
5 functional areas investigated:

- 6 • Head loss characteristics of various types of fibrous insulation by itself and in
7 combination with particulate matter (sludge).
- 8 • Head loss characteristics of other less common materials, such as containment
9 coatings, microporous insulation debris (Min-K and calcium silicate), in
10 combination with fibrous insulation debris.
- 11 • Head loss characteristics of reflective metallic insulation debris, by itself and in
12 combination with other debris such as fibrous and particulate matter.
- 13 • Head loss characteristics of insulation debris deposited on specific strainer or sump
14 designs.

15 Some of the previous difficulty in obtaining repeatable and comparable results lay in the testing
16 methodology. Having results that can be directly correlated with the realistic plant configurations
17 and arrangements, or that can be properly scaled to these, is important.

18 **E.3 HEAD LOSS CORRELATIONS**

19 Several different approaches and methodologies have been employed for predicting head loss
20 across debris beds. These approaches include theoretical or semi-theoretical relationships and
21 empirical relationships. As discussed below, some of the early empirical relationships, while
22 adequate for their intended purpose of predicting pressure drop across a single media debris bed,
23 are inadequate for predicting pressure drop across mixed debris beds. This inadequacy may have
24 contributed to some of the events challenging ECCS recirculation capability. It is important to
25 anticipate what debris may be transported to an ECCS screen, and to employ head loss
26 correlations valid for the combination of materials, anticipated debris characteristics, and
27 conditions expected. Different forms and approaches for head loss correlations are described in
28 the following paragraphs.

29 **Empirical Correlation for Fiber-Only Beds**

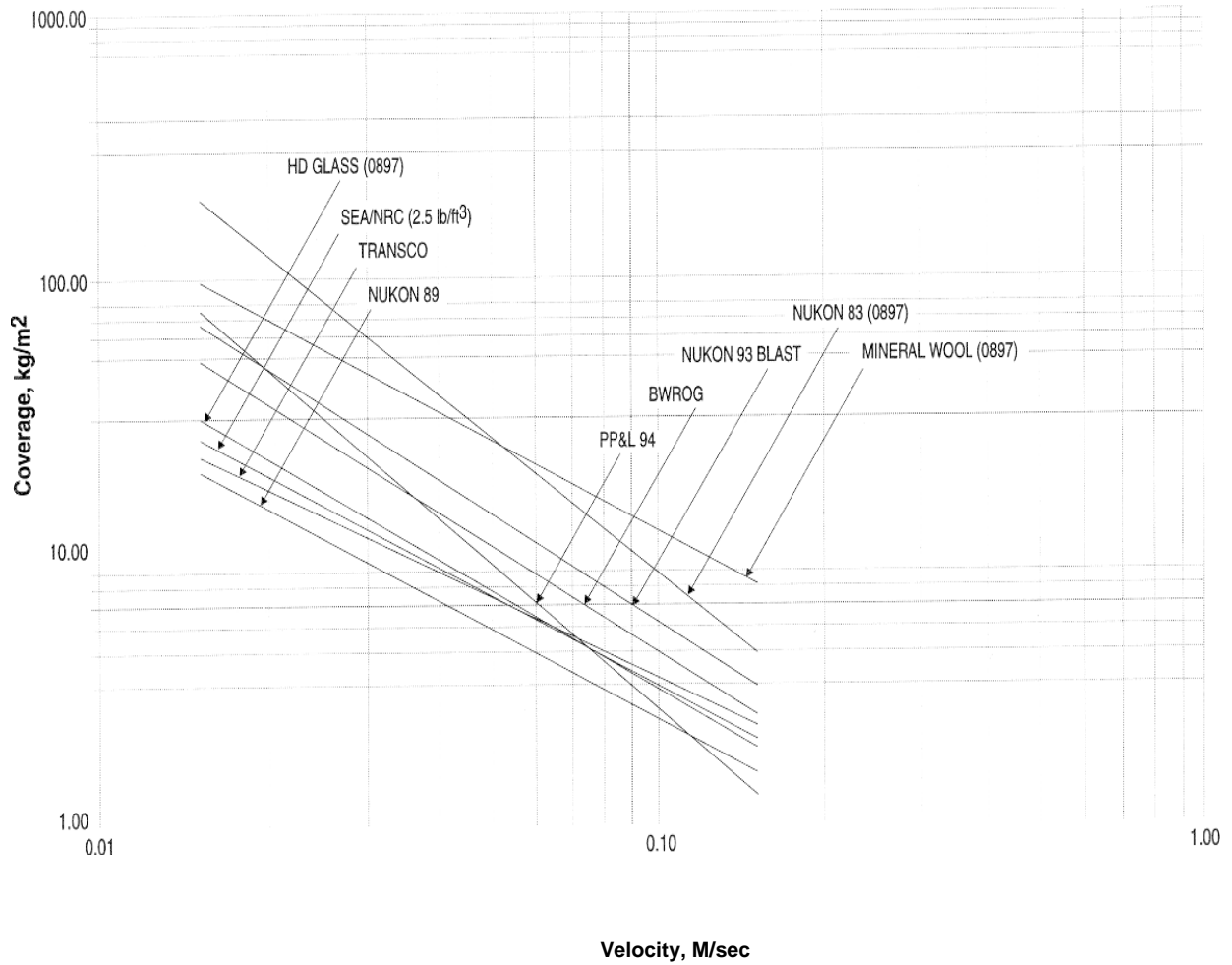
30 Early strainer or screen design methods typically assumed that the screen/strainer pressure drop
31 was primarily due to an accumulation of fibrous debris. For pure fiber beds, most studies
32 developed empirical relationships to relate velocity and bed theoretical thickness or fibrous
33 debris accumulation to strainer pressure drop. The relationships were usually of the following
34 form:

$$35 \quad \Delta H = aV^b e^c \quad (1)$$

1 where,

2 ΔH is strainer head loss (ft)
3 V is strainer approach velocity (ft/sec)
4 e is debris bed theoretical thickness (ft)
5 $a, b,$ and c are empirical constants determined in experiments

6 These relationships, together with engineering judgment and assumptions regarding the debris
7 generation, debris characteristics, and transport, provided the basis for design and sizing of the
8 strainers. Some attempts were also made to employ similar relationships to correlate
9 experimental data obtained for mixed beds. The various correlations developed for debris beds
10 formed of pure mineral wool beds, pure low-density fiberglass beds, and mixed beds formed of
11 fiber and sludge mixtures are contained in the summary material of Table E-2. The predictions of
12 the correlations for low-density fiberglass are illustrated in Figure E-1, which clearly illustrates
13 the variabilities and uncertainties associated with early correlations that apply only to the low-
14 density fiberglass tested. Other insulation materials may exhibit different head loss
15 characteristics.



1

2 **Figure E-1. Comparison of Available Head Loss Correlation for Low-Density Fiberglass**
3 **Material Plotted as Strainer Coverage Required to Develop 2 Meters Water ΔP for Various**
4 **Fibrous Materials**

1 U.S. NRC NUREG/CR-6224 Head Loss Model

2 To minimize some of the shortcomings previously listed, the U.S. NRC sought a semi-theoretical
3 approach for correlating the experimental data. Equation 2 is of a form containing two terms that
4 account for head loss in the laminar and turbulent flow regimes, derived from the
5 Kozeny-Carman and Ergun Equations as explained in Table 4-5.

$$6 \quad \frac{\Delta P}{t} = 3.55 S_v^2 (1 - \varepsilon)^{1.5} \left[1 + 57(1 - \varepsilon)^3 \right] \mu V + \frac{0.66 S_v (1 - \varepsilon)}{\varepsilon} \rho V^2 \quad (2)$$

7 where,

8	ΔP	is the pressure drop that is due to flow across the bed (dynes/cm ²)
9	t	is the height or thickness of the fibrous bed (cm)
10	μ	is the fluid dynamic viscosity (poise)
11	ρ	is the fluid density (g/cc)
12	V	is the fluid velocity (cm/sec)
13	ε	is the bed porosity
14	S_v	is the specific surface area (cm ² /cm ³)

15 This correlation has the following salient features:

- 16 • Head loss dependence on the type of fibrous insulation material (e.g., mineral wool
17 versus low-density fiberglass) can be handled directly by varying material
18 properties (fiber-specific surface area, fiber strand density, and material packing
19 density) in the equation. This eliminates the need for developing a separate
20 equation for each debris type.
- 21 • Head loss dependence on particulate can be handled directly by varying the bed
22 porosity.
- 23 • The same equation is valid for laminar, transitional, and turbulent flow regimes,
24 which maximizes its usage in the plant analysis.
- 25 • Head loss dependence on water temperature can be handled explicitly through the
26 use of flow viscosity in the equation.
- 27 • Compressibility effects can be handled by analysis.

28 A series of experiments was conducted by the U.S. NRC to obtain head loss data that can be used
29 to validate the correlation previously listed. The experimental data obtained from these tests
30 formed the most comprehensive head loss database for debris beds formed of Nukon and
31 corrosion products, encompassing an experimental parameter range of 3 mm to 10.2 cm for
32 thickness; 5 to 50 cm/sec for approach velocity; 0 to 60 for sludge-to-fiber mass ratios; and at
33 temperatures of 24° and 52°C. Detailed comparison of the correlation predictions with these

1 experimental data is presented in NUREG/CR-6224. This correlation was used for the plant
2 evaluation reported in NUREG/CR-6224 and has also been incorporated into the BLOCKAGE
3 computer code developed by the U.S. NRC.

4 The following limitations of this correlation are identified for the potential user:

- 5 • The correlation may not be applicable for nonuniform debris beds since the
6 correlation is developed based on the assumption that the debris forms a uniform
7 bed. This may limit equation applicability to very thin beds or thin beds formed on
8 specialized strainers.
- 9 • The correlation may not be applicable to thin fiber beds coupled with high sludge-
10 to-fiber mass ratios since nonuniform debris bed thicknesses, including open
11 spaces, were observed in the ARL experiments.
- 12 • Although this correlation is expected to provide an upper-bound estimate for the
13 head loss, these limitations and other factors presented in NUREG/CR-6224 should
14 be reviewed before using this correlation.
- 15 • As explained in subsection 5.1.6.3, debris bed loadings of microporous insulation
16 debris exceeding microporous-to-fiber mass ratio of 0.2 may result in somewhat
17 nonconservative results from the above NUREG-6224 correlation.

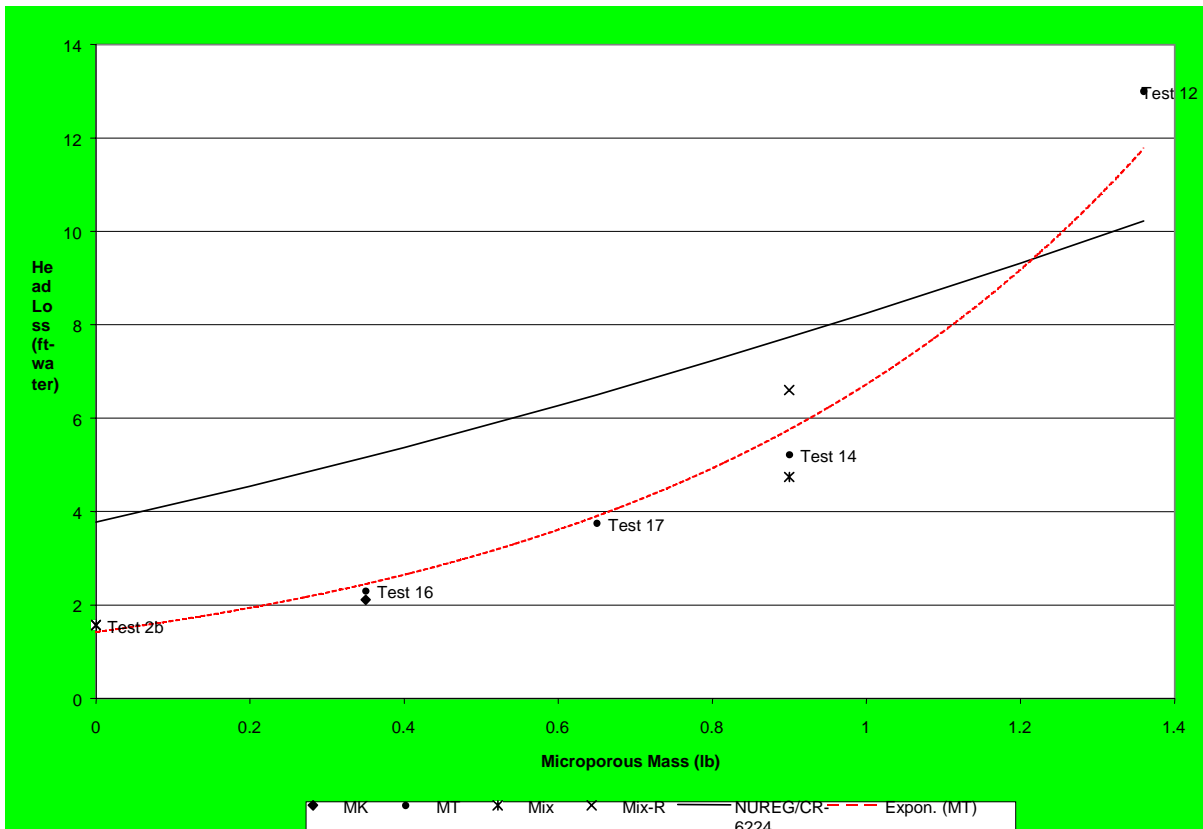
18 **Impact of Microporous Insulation Debris**

19 A postulated LOCA due to a high-energy pipe break could generate a mixture of fibrous and
20 microporous insulation debris that may be potentially transported to the ECCS pump intake
21 screens. Experiments were conducted to address the head loss behavior due to mixtures of
22 fibrous and microporous debris. In particular, these experiments considered several combinations
23 of microporous insulation debris (i.e., Min-K, Microtherm, Cal-Sil) mixed with fibrous
24 insulation debris and particulate debris.

25 The microporous tests showed that the contributions to head loss of microporous insulation could
26 be neglected when conditions yielded a microporous mass to strainer surface area ratio of
27 0.02 lb/ft^2 . Scaling of the experimental results to the prototypical conditions can be accomplished
28 by scaling to the actual installed strainers apportioning the microporous loads in the ratio of the
29 flows when more than one strainer is operational.

30 The microporous tests also showed that it is possible to use the NUREG/CR-6224 head loss
31 correlation to bound the observed test results for mixtures of fibrous and microporous insulation
32 debris when the microporous-to-fiber mass ratio is less than 0.2. For quantities of debris for
33 which the microporous-to-fibrous mass ratio exceeds 0.2, the head loss behavior appears to be
34 dominated by the microporous component, and the NUREG/CR-6224 head loss approximation is
35 no longer applicable.

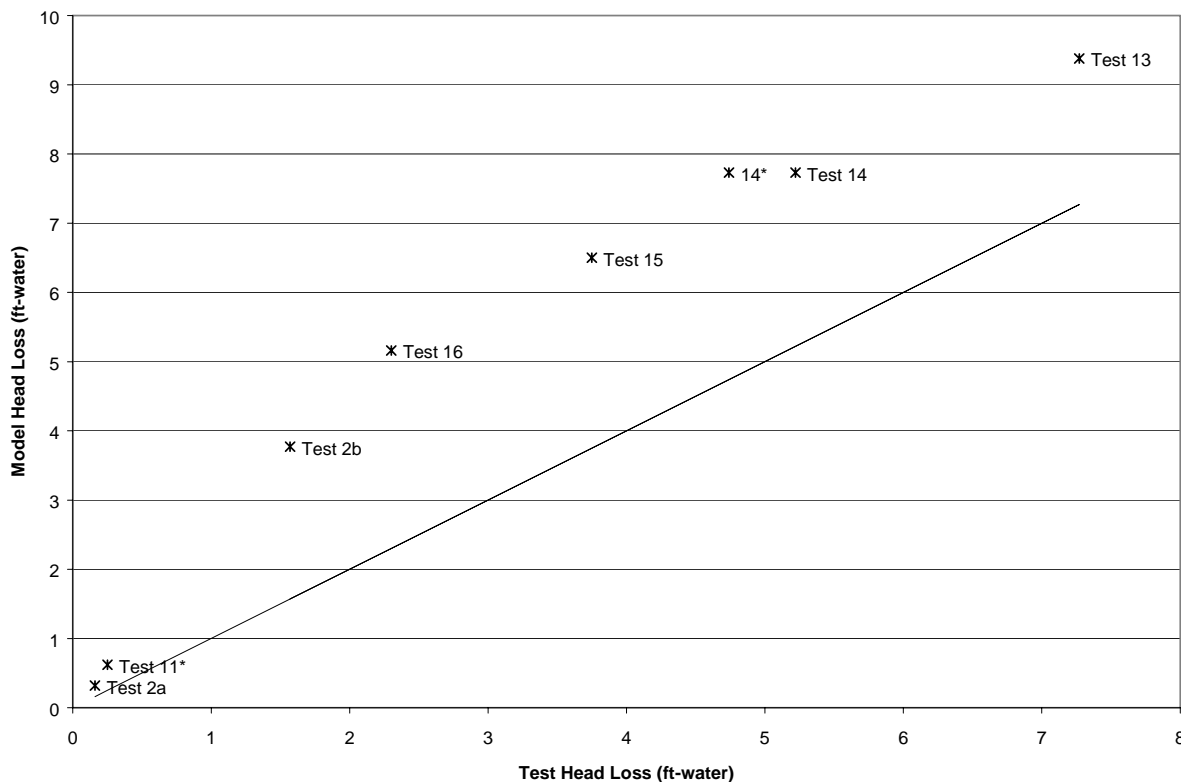
1 Use of the NUREG/CR-6224 head loss correlation to approximate the observed head loss
 2 behavior due to fibrous and microporous insulation debris requires the specification of a
 3 characteristic size and density of the microporous particles. Reasonable agreement with the
 4 observed head loss results is obtained when the microporous particulate matter debris is assumed
 5 to be in spherical particles, with a characteristic size of 5 μm and a density of 140 lb/ft^3 . With
 6 these parameters to characterize microporous particles, the NUREG/CR-6224 head loss
 7 correlation adequately bounds the observed test data when the microporous-to-fiber mass ratio is
 8 less than approximately 0.2. This comparison is shown in Figure 4-4, which presents the
 9 NUREG/CR-6224 head loss correlation and the measured head loss results for 6 pounds of fibers
 10 at a flow rate of 200 gpm (equivalent to an approach velocity of 0.09 ft/sec) and a water
 11 temperature of 60°F.



12
 13 **Figure E-2. Comparison between the NUREG/CR-6224 Head Loss Correlation and the**
 14 **Test Data for 6.0 lb of Fibrous Insulation Debris in the Test Tank**

15 As indicated in the figure, the NUREG/CR-6224 head loss correlation adequately bounds the test
 16 data when the microporous-to-fiber mass ratio is less than 0.2 and when the aforementioned
 17 parameters are used to characterize the microporous debris (i.e., size and density).

18 A comparison of the NUREG/CR-6224 head loss correlation with the test data for a
 19 microporous-to-fiber mass ratio less than 0.2, including a medium fiber load as well as the
 20 applicable test with simulated sludge, is presented in Figure E-3.



1

2 Note: The straight line corresponds to an ideal agreement with the test results.

3 **Figure E-3. Comparison between the NUREG/CR-6224 Head Loss Correlation and the**
 4 **Test Data when the Microporous-to-Fiber Mass Ratio in the Test Tank is Less than 0.2**

5 As indicated in Figure E-3, the proposed model of considering that microporous insulation debris
 6 may be treated as particulate matter debris, with the NUREG/CR-6224 head loss correlation,
 7 bounds the test data when the microporous-to-fiber mass ratio in the tank is less than 0.2.
 8 Consequently, estimation of head losses due to mixtures of debris with microporous insulation
 9 debris can treat the microporous insulation as a particulate matter debris in the NUREG/CR-6224
 10 head loss correlation for fibrous debris, provided that the microporous-to-fiber mass ratio in the
 11 debris bed does not exceed 0.2.

12 **U. S. BWROG Characterization of Combined Debris Head Loss**

13 The U.S. BWROG, while conducting combined debris testing to establish the bases for resolution
 14 of the ECCS suction strainer plugging issues, has observed phenomena that may have significant
 15 implications for potential resolutions of the ECCS suction strainer issue. In general, the BWROG
 16 observations indicate increasing head losses when both fiber loading and corrosion product
 17 loading on the strainer are increased together, which is what would be anticipated. A second and
 18 more significant observation was not initially expected. If the amount of fibrous debris in the bed
 19 is decreased while the amount of particulate material is held constant, the head loss could
 20 increase (depending on the ratio of the mass of corrosion products to the mass of fiber) rather

1 than decrease as might be initially thought. This behavior was previously suggested by
2 Vattenfall.

3 While this phenomenon seems counterintuitive, this finding is consistent with other European
4 experiments. As demonstrated during the Perry events and confirmed by subsequent testing, only
5 a thin bed of fiber is required on the surface of a flat-plate strainer to effectively filter out fine
6 particulate materials that would have otherwise passed through the strainer. The BWROG testing
7 program demonstrated that the highest head losses occur with thin layers of fiber and high ratios
8 of corrosion product mass to fibrous debris on flat-plate strainers.

9 Physically, a given amount of particulate material results in debris beds that can become
10 increasingly compact and decreasingly porous as the amount of fiber present in the bed
11 decreases. The end result is that a fiber bed just thick enough to bridge all of the strainer holes
12 combined with an inventory of fine particulate materials can result in a very large head loss.
13 Based on the testing performed and current understanding of the likely physical causes, these
14 phenomena would not be expected to proceed beyond the point where the layer of fibrous
15 material is insufficient to fully bridge all of the strainer holes. These observations were made
16 during extensive testing both on fiber only and on debris beds comprising fiber and corrosion
17 products. The iron oxide corrosion products used for these tests had a larger average particle size
18 than that typically present in U.S. BWR suppression pools. Use of the larger-size particulate
19 material was shown to result in a conservative estimate of the combined debris head losses, as
20 larger particles are more likely to be captured in the fibrous bed. The following head loss
21 correlation was documented in the BWROG URG (Reference 54) (Note: Other correlations
22 were developed by replacement strainer vendors.)

$$23 \quad \Delta h = K_h \mu U t / (\rho g d^2) \quad (3)$$

24 where,

25 Δh is strainer head loss, ft of water
26 μ is viscosity, lb-sec/ft²
27 U is strainer approach velocity, ft/sec
28 t is fiber bed thickness, ft
29 ρ is water density slug/ft²
30 g is gravitational constant, 32.2 ft/sec²
31 d is inter-fiber spacing, ft

32 This equation has been simplified to:

$$33 \quad \Delta h = a + bU \quad (4)$$

34 where a and b are coefficients dependent on the ratios (Ms/Mf) of different masses of solids (e.g.,
35 corrosion products, paint chips, rust flakes, sand, cement dust, calcium silicate, etc.) and fibrous
36 materials assumed to collect on the debris bed.

1 A significant aspect of this section is that a large head loss can occur with relatively small fibrous
2 loading in combination with a particulate inventory, and that the resolution options must be able
3 to manage or prevent unacceptable strainer head losses. Equations 3 and 4 and the BWROG
4 URG methodology were developed by the U.S. BWROG for specific conditions and should,
5 therefore, be used with caution and reviewed for applicability by the user.

6 Moreover, the NRC Safety Evaluation Report for the URG methodology noted in Section ES.7,

7 *... the staff finds that the head loss correlations in the URG are unreliable and*
8 *incomplete for plant analysis and, therefore, is unacceptable. The staff strongly*
9 *recommends that utilities use vendor-provided data to qualify strainer designs,*
10 *rather than relying on the correlations and calculation procedures specified in the*
11 *URG.*

12 **Characterization of Head Loss Due to Reflective Metallic Insulation**

13 Many plants have some reflective metallic insulation (RMI) installed, and there has been
14 significant interest in the behavior of this material. Experiments have been performed to
15 determine how it and other materials react to blast and jet forces, and its transport characteristics.
16 Head loss testing of debris beds comprising RMI, or of mixed beds containing RMI, has been
17 conducted by several organizations, as described in detail in Table E-2. The topic of RMI debris
18 bed head loss has initiated some disagreement, and it would appear that much of the lack of
19 agreement stems from RMI debris shape, bed morphology, and transport characteristics
20 fundamental to the head loss experiments. For one to evaluate the effect of RMI, the shape and
21 form of RMI reaching the bed, and the predicted morphology of the bed under accident
22 conditions should be carefully evaluated to ensure that the testing and derived relationships
23 properly represent the real situation.

24 The following observations provide the basis for the method of accounting for RMI contribution
25 to debris bed head loss in the U.S.:

- 26 1. The transport characteristics for RMI may be different than other debris, and must
27 be accounted for in predicting the debris bed formation. Depending on the pool
28 turbulence and approach velocities, RMI deposition may not be uniform.
- 29 2. If RMI does transport and is deposited on screens/strainers, it will produce head
30 loss. The head loss developed is highly dependent on the type of RMI debris. For
31 example, if a large, intact sheet of metallic foil is deposited over the screen or
32 strainer, it will reduce the flow area significantly and increase the velocity and head
33 loss in the remaining flow area. Based on various results from debris generation
34 testing, RMI debris is expected to be small and crumpled in form, as opposed to
35 large, intact sheets. The head loss characteristics of this type of RMI debris range
36 from benign to small in comparison with that expected from combined
37 fiber/particulate beds.

1 The BWROG has recommended, in its URG, use of the following equation for determining RMI
2 bed head loss (the equation is valid for head losses under ~10 feet H₂O):

$$3 \quad \Delta h = K_p U^2 t_p \quad (5)$$

4 where,

5 Δh is head loss, ft of water
6 K_p is a constant depending on the type of RMI and strainer
7 U is the approach velocity, ft/sec
8 t_p is the projected RMI debris bed thickness

9 A similar relationship has been suggested by the NRC:

$$10 \quad \Delta P \propto \frac{S_v(1-\epsilon)}{\epsilon^2} U^2 \quad N \propto \frac{L_1 * L_2}{K_t^2} U^2 (A_{\text{foil}} / A_{\text{str}}) \quad (6)$$

11 where,

12 ΔP is head loss
13 L, S are foil dimensions
14 K is inter-foil channel size
15 U is approach velocity
16 N is number of foil layers

17 Where there is combined debris consisting of fibrous material, particulate matter or sludge, and
18 RMI, the head loss due to the fibrous and particulate material are expected to dominate. Testing
19 of BWR prototypic strainers has indicated that RMI does not cause significantly different head
20 losses than those caused by fibrous debris and sludge only. The NRC and BWROG research does
21 not indicate the presence of an autocatalytic or synergistic effect between RMI and other debris
22 beds similar to combined fibrous and particulate beds. For mixed RMI and fiber beds, the NRC
23 approach to consideration of RMI head loss is that it should be added (summed) to the head
24 losses expected from other (fibrous and particulate) debris unless it can be demonstrated that this
25 conservative approach is not appropriate. This recognizes and accounts for the NRC staff
26 conclusion that the head loss of a fiber plus corrosion product bed does not bound the head loss
27 of a fiber, corrosion product, and RMI debris bed in all situations.

28 Other investigators have reported results and conclusions that differ from the above due to
29 considerations associated with the structure of metallic debris beds. The bed structure, as alluded
30 to before, will have a significant impact on the head loss. For example, consider a bed of metallic
31 foils where most of the foils are arranged parallel to the flow direction. One might expect that
32 relative head loss resulting from this configuration with or without other material would be less
33 than other configurations. Consider a bed where most of the foils are deposited perpendicular to
34 the flow. This type of bed configuration will be subject to compression effects, and combined
35 debris would also tend to increase the head loss and bed compression. The realistic situation

1 would probably exist between these two extremes. As previously stated, the bed structure
 2 depends on many factors including its shape as generated during the LOCA event, how it is
 3 transported (tumbling on floor versus mid-stream suspension), and its formation sequence
 4 (mixed deposition of insulation and other debris, tumbling up from bottom or curb, etc.). Again,
 5 it is important to carefully consider the plant-specific situation to develop realistic models.

6 Another form of RMI head loss correlation takes into consideration the pressure drop in RMI
 7 debris beds with gap or bypass:

$$8 \quad \frac{\Delta p}{\frac{\rho w_o^2}{2}} = f_{(R)} \frac{nW}{D} \quad (7)$$

9 where,

10 Δp is the pressure drop
 11 ρ is the fluid density
 12 w_o is velocity
 13 $f_{(R)}$ is friction factor
 14 n_w is path length of fluid traveled in the bed; n is the number of foil layers and W the
 15 foil lateral length
 16 D is the width of the flow channel; depth of foil crumpling

17 This relationship assumes that pressure drop in a metallic bed behaves analogously to pipe flow.
 18 The friction factor, f, depends on bed morphology (structure), and may also contain dependency
 19 on debris surface characteristics such as relative roughness, in addition to the Reynolds number,
 20 and must be determined experimentally. The correlation is presently limited by the following
 21 assumptions:

22 The debris has uniform dimensions.

- 23 • The debris bed area is independent of thickness.

24 While investigating the RMI debris head losses, it was observed that the ratio of maximum to
 25 minimum head loss for different configurations (flatter RMI debris perpendicular to flow versus
 26 parallel to flow) can vary by two or three orders of magnitude.

27 It should be noted that the variability of different vendor products (e.g., dimpled foils, waffle
 28 patterns, or smooth patterns) suggests caution and review of product lines before extrapolating
 29 results. In addition, some experimental results indicate that mixtures of foil pieces and fibrous
 30 debris can result in significantly higher head losses than would be derived from summing the
 31 individual contributions.

1 **Related Methodologies**

2 Several companion methodologies have been developed utilizing the research results and
 3 methods discussed above. These methods have been primarily developed for use in calculating
 4 the pressure drop across replacement suction strainers, and are discussed in Table 4-5. Typical of
 5 these methodologies is one developed that utilizes dimensional analysis for determination of
 6 head loss and has been further enhanced to account for bed compression and different strainer
 7 geometrical configurations such as would be present in a stacked disc or star strainer. The basic
 8 equation is of the following form:

$$9 \quad \Delta H A_s^2 \rho / QM \left(v / d_{if}^2 \right) [1 + k Re] = f(\eta) \quad (8)$$

10 where,

11	ΔH	is the head loss
12	A_s	is the surface area
13	ρ	is the bed density
14	Q	is volume flow
15	M	is mass of fiber M_f and mass of sludge
16	M_s	is kinematic viscosity
17	d_{if}	is inter-fiber spacing
18	k	is a constant
19	Re	is the Reynolds number, $Re = (Q/A_s)d_{if}/v$
20	η	is M_s/M_f

Table E-2. Summary of Head Loss Tests

Sponsor	Test Facility		Date	Report Reference
BWROG, GE Nuclear Energy	Continuum Dynamics, Inc. at EPRI NDE Center, Charlotte		November 1996	54
Variables Studied	Ranges	Results/Relationships	Comments	
Purpose of Tests: Full-scale tests to obtain pressure loss and performance data on different strainer types as a function of debris type, quantity, flow rate, and time		Qualitatively, this testing showed that passive strainers had been identified that show improved performance over the original strainers. These strainers can collect significant amounts of fibrous insulation and corrosion products with acceptable head loss at the flow rates of interest for BWR ECCS.	An extensive matrix of tests was performed to obtain strainer performance information that is too extensive to summarize here. Consultation of the reference is suggested to obtain specific information.	
Materials Tested: Nukon, Kaowool, Tempmat, calcium silicate, BWR corrosion product sludge, RMI-various				
Insulation Preparation: See reference, per NUREG-6224 recommendations.				
Material Introduction Method: See reference.				
Coverage: Various, see reference.				
Approach Velocity: Various, see reference.				
Maximum Head Loss: 500 in. H ₂ O				
Temperature: 60-86°F				
pH: 8-10				

Table E-2. Summary of Head Loss Tests (Cont'd)

Sponsor	Test Facility		Date	Report Reference
Commonwealth Edison Company	Continuum Dynamics, Inc., Princeton, N. J.		July 1997	55
Variables Studied	Ranges	Results/Relationships	Comments	
Purpose of Tests: Evaluation of the effects of paint chips on sump strainer head loss. Determination of head loss across the sump screen resulting from the buildup of paint chips.		The effect of paint chips by themselves on head loss was minimal.	Most paint chips remained on tank floor and did not reach strainer. When flow was stopped, chips on screen fell off.	
Materials Tested: Epoxy paint chips, Ameron/Amercoat 90HS by itself on screens, no other materials.				
Material Preparation: Dry paint peeled from plastic sheet, then broken up by hand or in a household blender.				
Material Introduction Method: Chips were presoaked to avoid floating, and added to test tank near diffuser.				
Coverage	1000 to 4700 ft ² paint chips on 28 ft ² screen, scaled			
Approach Velocity: Prototypical, ~0.72 ft/sec.				
Maximum Head Loss	0.2 inches water			
Temperature	Ambient			
pH	Ambient			

Table E-2. Summary of Head Loss Tests (Cont'd)

Sponsor	Test Facility		Date	Report Reference
Northeast Nuclear Energy Company, Millstone Unit 1	Continuum Dynamics, Inc.		February 1999	56
Variables Studied	Ranges	Results/Relationships	Comments	
Purpose of Tests: To evaluate the amount of coating, fibrous, and RMI debris that can be transported to a PWR sump screen during post-LOCA recirculation, and to measure the resultant head loss across the debris bed. The effect of boric acid on zinc chips was also evaluated.		Paint chips with boric acid: with pH at 6.0 and 1" to 2" bed of paint chips at V = 0.25 ft/sec, no movement of chips or increase in head loss. Similar results for paint chips by themselves, no boric acid. 0.115 ft ³ Nukon fiber placed ~20 ft from sump screen. Flow started at 0.2 ft/sec, approached to 1.5 ft from screen and stopped. No change in head loss. Ten times amount of fiber placed in tank, 20 ft from screen with velocities up to 0.25 ft/sec with none on screen, no increase in head loss. Even with fiber moved directly in front of sump, no motion along floor or increase in head loss. Further addition of RMI did not result in debris movement or accumulation on screen. Paint chips added during flow resulted in some transport to screen, but resulted in a head loss of <1.32 inches water.	Paint chips, fiber, and RMI on the sump floor at the initiation of flow are unlikely to transport to the sump and generate any measurable head loss. Addition of boric acid does not increase the likelihood of paint chip transport.	
Materials Tested: Phenolene 305 epoxy and carbozinc 11 inorganic zinc primer, Nukon fibrous debris, 2-mil stainless RMI, boric acid.	Size of paint: <1/8"-13% 1/8-1/4"-40% 1/4"-1/2"-39% 1/2"-3/4"-7%			
Material Preparation	Paint applied to plastic, sheets, cured and peeled off, shredded into chips. Nukon shredded into small pieces <1/2", classified as NUREG 6224 types 3, 4, and 5. RMI cut into 6", 3", 1", and 3/8" squares and then crumpled.			
Material Introduction Method	Wetted debris added to tank (full-scale segment of screen) and allowed to settle, pumps then started.			
Coverage	500 ft ² equiv. Paint, 0.115 ft ³ fiber, 2.5 ft ² RMI in test matrix.			
Approach Velocity	0-0.25 ft/sec			
Maximum Head Loss	1.3 in. H ₂ O			
Temperature	Ambient			
pH	> 6.0 with boric acid			

Table E-2. Summary of Head Loss Tests (Cont'd)

Sponsor	Test Facility		Date	Report Reference
Detroit Edison/Duke Engineering and Services	ITS Corporation at EPRI NDE Center		October 14, 1997 Preliminary	57
Variables Studied	Ranges	Results/Relationships	Comments	
Purpose of Tests: To characterize the impact of Min-K insulation on prototype ECCS suction strainers.		Min-K bed is different than fiberglass. Debris bed was <1/4" thick, uniform. Debris penetrated and plugged suction strainer holes. The debris bed did not resemble long fiber over the holes.		
Materials Tested: Min-K core material, silica and titanium dioxide, and sludge.		Addition of sludge did not produce significantly higher head loss than with Min-K by itself.		
Material Preparation	Min-K core material supplied in loose powder form, and sludge stimulant developed by NRC.	Head loss seems to continue to increase with time, even after "steady state" was achieved.		
Material Introduction Method	Flow established, Min-K slurry introduced into tank. If sludge used, it was first introduced, followed by Min-K.			
Coverage	0-96 lb Min-K, 0-17 lb sludge			
Approach Velocity	6350 gpm flow rate			
Maximum Head Loss	158 inches water			
Temperature	Ambient, 78°F			
pH	Neutral, tap water			

Table E-2. Summary of Head Loss Tests (Cont'd)

Sponsor	Test Facility		Date	Report Reference
New York Power Authority, James A. Fitzpatrick (JAF) Nuclear Power Plant	ITS at Alden Research Laboratory; 1:2.4 scale model of BWR Mk 1 Suppression Pool		Spring 1999	58
Variables Studied	Ranges	Results/Relationships	Comments	
Purpose of Tests: Evaluate replacement strainers for JAF; head loss data for microporous insulation was sparse and suggested higher head losses than for fiber beds.		NUREG/CR-6224 conservatively modeled fibrous material. Min-K head loss is greater than that for equivalent amount of microtherm.	Microporous applies to either Min-K or Microtherm.	
Materials Tested: Fibrous: Nukon, Temp-Mat, and Knauf; Min-K; Microtherm.		NUREG/CR-6224 conservatively models head losses for microporous debris microporous to fiber mass ratios <0.2.		
Material Preparation				
Material Introduction Method	Debris mixed with water to form slurry, added to test tank; additional debris added in steady-state plateaus: Fibrous only, microporous only, microporous and fiber	Cal-Sil head loss characteristics similar to Min-K and Microtherm.		
Coverage	0-6 lb fiber, 0-1 lb Min-K, 0-1 lb microtherm			
Approach Velocity	~0.096 ft/sec			
Maximum Head Loss	~13 ft H ₂ O			
Temperature	Ambient			
pH	Ambient			

Table E-2. Summary of Head Loss Tests (Cont'd)

Sponsor	Test Facility		Date	Report Reference												
USNRC	Alden Research Laboratory		December 1995	59												
Variables Studied	Ranges	Results/Relationships	Comments													
Purpose of Tests: Determine the pressure loss characteristics of Thermal Wrap insulation debris with and without iron oxide particles to simulate BWR suppression pool sludge.		No significant differences were found for fibrous insulation head losses between: Thermal Wrap [®] (Knauf-Transco) and Nukon (Owens Corning-PCI).	Higher water temperature reduces head loss because of viscosity effects. This testing was similar to that conducted on Nukon insulation debris by Alden Laboratory and reported in June 1995.													
Materials Tested: Thermal Wrap insulation debris, simulated iron oxide sludge, and paint chips		Head loss increased with bed thickness from 3 ft H ₂ O for 0.25" to 34 ft for 4" without sludge. Head loss also increased for increasing sludge to insulation mass ratios; for 1" bed by a factor of 70 from 0 sludge to 7.5 ratio.														
Material Preparation	Insulating blankets were heat-treated and shredded in a leaf shredder.	Variation in sludge particle size or the addition of paint chips had no measurable effect on head loss.														
Material Introduction Method	Sludge added to test loop, well mixed, then insulation added at once.															
Coverage	Fibrous insulation thickness 0.25-4 in., size classes 3 & 4; and 0-30 sludge-to-fiber mass ratios.															
Approach Velocity	0.15 ft/sec during bed formation; 0.15-1.5 ft/sec test															
Maximum Head Loss	~55 ft															
Temperature	125°F															
pH	Not investigated															

Table E-2. Summary of Head Loss Tests (Cont'd)

Sponsor	Test Facility		Date	Report Reference
Fortum Engineering, Ltd			May 20, 1999	60
Variables Studied	Ranges	Results/Relationships	Comments	
Purpose of Tests: To study the strainer differential pressure caused by different insulation types when subjected to the same debris generation, testing, and sump configuration.		Corrected differential pressure for this demonstration 67.5, 10, and 33 kPa for the three insulation types listed under materials. Transportable fractions of debris were 62, 34, and 100%, respectively.		
Materials Tested: Fine fiber (Al-Si) insulation, coarse glass fiber insulation, and Si-Ca mineral insulation.	8 kg 27 kg 5 kg			
Material Preparation	Insulation was heat- treated at 300°C for 48 hours, and subjected to steam/water jet impingement; resulting debris was collected, examined.			
Material Introduction Method	After examination, the material was introduced into the sump test facility.			
Coverage				
Approach Velocity	18-25 mm/sec			
Maximum Head Loss				
Temperature	50°C			
pH	H ₃ BO ₃ conc. 12 g/kg H ₂ O			

Table E-2. Summary of Head Loss Tests (Cont'd)

Sponsor	Test Facility		Date	Report Reference
U. S. Nuclear Regulatory Commission	Alden Research Laboratory		May 1996	61
Variables Studied	Ranges	Results/Relationships	Comments	
Purpose of Tests: To provide basic insights into the behavior of RMI debris under LOCA conditions, by itself and in combination with other debris.		Introduction of prototypical RMI debris in the presence of fiber and sludge does not cause significantly different head losses than the head losses observed with only fiber and sludge loadings. During testing, RMI debris, when intermixed with fibrous debris and sludge, appeared to decrease head losses compared to similar conditions without RMI debris. Head losses for RMI without any other debris were relatively small, but increased with increasing mass of RMI. RMI debris size had no practical effect on head losses for a given mass/unit area of strainer.		
Materials Tested: Diamond Power Mirror insulation, Nukon insulation.				
Material Preparation	Prototypical RMI for sedimentation and head loss testing was generated by Siemens AG/KWU in Karlstein am Main, Germany.			
Material Introduction Method	Sludge added first, then fibrous insulation and RMI, alternatively.			
Coverage	Variable			
Approach Velocity	0.15-1.5 ft/sec			
Maximum Head Loss	~37 ft H ₂ O			
Temperature	125			
pH	Not investigated			

Table E-2. Summary of Head Loss Tests (Cont'd)

Sponsor	Test Facility		Date	Report Reference
Commonwealth Edison, LaSalle Station	Duke Engineering and Services at EPRI, Charlotte, N. C.		June 1998	62
Variables Studied	Ranges	Results/Relationships	Comments	
Purpose of Tests: To obtain fiber and aluminum RMI data with an actual replacement strainer under prototypic conditions.		Measured head loss confirmed an approach velocity squared relationship.	Measured head loss for RMI debris was found to be a strong function of the process of debris deposition or accumulation on the strainer. "Shepherding" debris into the strainer suction flow field resulted in higher head losses than more normal processes.	
Materials tested: Nukon fibrous debris stimulant, 1.5-mil aluminum debris stimulant.		A synergistic effect of RMI and fibrous debris was observed resulting in head losses greater than adding each constituent's head loss.		
Material Preparation	Nukon shredded using methodology from NUREG-6224. Al RMI prototypical debris was generated at CEESI. The test debris was developed based on the generation experiments, limited in size (for transport), and crumpled.			
Material Introduction Method	Incremental RMI addition to operating system, and addition to tank followed by initiating system operation. RMI and fiber added together in tank followed by initiation of system operation.			
Coverage	Limited by test d/p			
Approach Velocity				
Maximum Head Loss	8.17 ft H ₂ O			
Temperature	Nominal ambient			
pH	Not investigated			

Table E-2. Summary of Head Loss Tests (Cont'd)

Sponsor	Test Facility		Date	Report Reference
Finnish Centre for Radiation and Nuclear Safety (STUK)	STUK		May 1999	63, 64
Variables Studied	Ranges	Results/Relationships	Comments	
<p>Purpose of Tests: To shed light on the physical mechanisms that induce flow resistance in purely metallic insulation debris beds, to quantify the influence of bed structure on flow resistance, and develop an approach to identify and quantify facility-related distortions.</p>		<p>Pressure drop caused by pure metallic insulation debris bed is strongly dependent on bed structure. It appears that this factor is more important than the characteristics of the debris. Minimal resistance is found when the debris is aligned with the streamlines, and maximum resistance is found with all debris perpendicular to the streamlines.</p>	<p>The raw data show that:</p> <ul style="list-style-type: none"> • Orderly debris bed behavior is qualitatively similar on a strainer in a pool and in a test tube section. • With debris perpendicular to flow, flow is purely turbulent (as expected); with debris parallel to streamlines, laminar conditions can be achieved. • The ratio of maximum to minimum head loss for different configurations (debris bed morphologies) of the same debris can be as high as 160 (not correcting for edge effects). 	
<p>Materials Tested: DARMET panel insulation.</p>				
<p>Material Preparation</p>	<p>Simulated debris, cut DARMET inner foil, 16 x 2.5 cm strips.</p>			
<p>Material Introduction Method</p>	<p>Strips laid on net into the test section in geometry desired.</p>			
<p>Coverage</p>	<p>12 layers parallel, 5 layers perpendicular, 10 layers perpendicular</p>			
<p>Approach Velocity</p>	<p>Variable</p>			
<p>Maximum Head Loss</p>	<p>Consult reference</p>			
<p>Temperature</p>	<p>50°C, 30°C, 30°C, not controlled</p>			
<p>pH</p>	<p>Not investigated</p>			

Table E-2. Summary of Head Loss Tests (Cont'd)

Sponsor	Test Facility		Date	Report Reference
Swedish Nuclear Power Inspectorate	Studsvik Material Corporation		January 1995	65
Variables Studied	Ranges	Results/Relationships	Comments	
<p>Purpose of Tests: The objective of the project is to ascertain if there is a risk of coagulation of debris particles or fibers that could result in strainer clogging.</p>		<p>pH at the “isoelectric points,” where the particle surface is uncharged, is at low value (pH <4) for most materials and some materials (iron oxide, fiberglass, minileit) show a tendency toward coagulation at this pH. SEM investigation of filtered material does not indicate a clear tendency toward coagulation at the isoelectric points. Mineral wool can possibly be a bigger problem for filtration than fiberglass. Small suspended particles are more problematic than large ones. Corrosion products of iron and biological slime can cause rapid pressure drop. Boronic acid can have an effect by changing the external chemical conditions for filtration of small particles.</p>		
<p>Materials Tested: Magnetite, iron oxide hydroxide, fiberglass, mineral wool, caposil, minileit, concrete, primary coloring, and biological slime.</p>				
<p>Investigation: Tests and experiments were conducted to determine electrophoretic mobility, coagulation tendency, calculation of ζ-potential, and appearance/size of particles and fibers.</p>				

Table E-2. Summary of Head Loss Tests (Cont'd)

Sponsor	Test Facility		Date	Report Reference
CANDU Owners Group/Ontario Power Generation	Ontario Power Generation		October 1999	66
Variables Studied	Ranges	Results/Relationships	Comments	
Purpose of Tests: Available head loss correlation did not cover parameters of interest; material types, 90-day mission time, pH transient, and velocities.		NUREG-6224 underestimates head losses for measured short-term pressure drop.		
Materials Tested: Fiberglass, calcium silicate, paint, dirt, concrete, rust.		Iron oxide and calcium silicate short-term results similar on volumetric basis.		
Material Preparation		Calcium silicate beds show a tendency to increase head loss for an extended period of time.		
Material Introduction Method				
Coverage	1 to 14-inch-thick beds of fiberglass and fiberglass/particulate mixtures.			
Approach Velocity	0.025-0.41 ft/sec fibrous material; 0.025-0.06 ft/sec mixtures			
Maximum Head Loss				
Temperature	40°C, 60°C			
pH	7 (most), 10, 10.7			

1

Table E-2. Summary of Head Loss Tests (Cont'd)

Sponsor	Test Facility		Date	Report Reference
KAEFER Isoliertechnik, Bremen, Germany	Bremen Polytechnic Department of Naval Architecture and Ocean Engineering – Circulation Water Channel		July 1995	N/A
Variables Studied	Ranges	Results/Relationships	Comments	
Purpose of Tests: Generic tests to quantify head loss of different insulation materials as a function of debris thickness, flow velocity, and water conditions (temperature and chemistry).		The experiments with the relevant material types (fiber shreds, mattress debris, foil bulks) showed a pronounced increase in head loss with the loading thickness of the screen and the flow velocity. For a flow velocity of 0.06 m/sec and a loading thickness of 300 mm, head loss for fiber-type material is typically on the order of 100 kPa. For these materials, the head loss tends to increase for higher pH values. However, the opposite was found for glass fiber material. In general, the higher temperatures reduced the head loss considerably, i.e., roughly by half. In contrast, the metal foil fragments showed very small head loss values.	The results define a general and unique database for head loss of a variety of insulation materials.	
Materials Tested: Mattress-type insulation material (NGI type 2, mineral wool), cassette-type insulation material (fibre glass, mineral wool, reflective foils).	Bed thickness up to 300 mm in 8-in. circulation pipe with screen.			
Material Preparation: See reference.				
Material Introduction Method	Direct loading of a screen (0.25-in. mash size, 1-mm wire thickness).			
Coverage				
Approach Velocity	2-7 cm/sec			
Maximum Head Loss	See detailed reports.			
Temperature	18° and 49°C (64° and 120°F)			
pH	Two different water qualities: pH 7.0, boric acid 1800 ppm, sodium 84 ppm pH 9.2, boric acid 1800 ppm, sodium 2400 ppm			

2